Nanosized Transition Metal Spinels with High Surface Areas from Zeolite Precursors

Wolfgang Schmidt* and Claudia Weidenthaler

Max-Planck-Institut für Kohlenforschung, Kaiser-Wilhelm-Platz 1, D-45470 Mülheim, Germany

Received July 17, 2000. Revised Manuscript Received September 27, 2000

Spinel particles with sizes in the nanometer range having high surface areas are obtained by the calcination of transition metal exchanged zeolites. The spinel crystallites grow within an amorphous silica matrix, formed by the collapse of the zeolite framework. Dissolution of this matrix leads to the high surface area spinels. The compositions of the zeolites, as well as the calcination conditions, have an influence on the type of phases formed and on the properties of the phases. The adjustment of these conditions enables control of the size of the spinel particles.

Introduction

Transition metal spinels are of importance in various fields due to their high thermal resistance and specific catalytic and/or electronic properties. They are used in sensor and semiconductor technology as well as in heterogeneous catalysis.[1−4] High surface areas of solid particles are of predominant importance for processes taking place at the phase boundary between solid particles and a liquid or gas phase. Thus, spinels with high surface areas are of special interest for sensors and catalytic processes. Usually high surface areas go along with small particle sizes of the solid. Spherical particles of transition metal spinels must be smaller than 14 nm in diameter to achieve specific surface areas over 100 $m^2\ g^{-1}$.

Spinels with specific surface areas in the range of 100 $m^2\ g^{-1}$ are easily obtained by coprecipitation of metal hydroxides followed by calcination to form the spinel.[5−8] Using this method, aluminum oxide crystallizes quite often as byproduct, and in many cases the high surface areas of the products are caused by the aluminum oxide rather than by the spinel particles. Coprecipitation of hydroxides is a common method in catalyst preparation, but it requires large efforts to ensure a homogeneous material with uniform properties, e.g. in particle size, composition, or homogeneity, is formed. A homogeneous distribution of the metal components within the hydroxides is crucial for the crystallization of small spinel particles during the calcination. Materials with specific surface areas up to 250 $m^2\ g^{-1}$ are formed by calcining precursors obtained by sol−gel processes.[9−11] Using this method, the elements become uniformly distributed during the gel formation step. Disadvantages of the sol−gel process are the relative high costs of the metal alkoxides and the release of large amounts of alcohol during calcination requiring special safety precautions. The preparation of spinels by other processes, such as chemical vapor deposition[12−14] or from microemulsions,[15−17] is also possible but not very suitable if larger amounts of materials are needed as for catalytic processes. Colyer et al. observed the crystallization of spinel phases during the calcination of Zn^{2+}- and Co^{2+}-exchanged zeolite A.[18−20] In our work, where we investigate the thermal stability of three different zeolites exchanged with various transition metal cations, these results are confirmed. From that starting point, we developed an easy, reproducible, and cheap method for the preparation of transition metal aluminates with high surface areas. This novel method is demonstrated by the preparation of $CoAl_2O_4$, $NiAl_2O_4$, and $ZnAl_2O_4$ spinels.

Experimental Section

Ion-exchanged zeolites were obtained by stirring 5 g of the respective zeolite in 250 mL of 0.1 M salt solution at 70 °C

(1) Shimizu, Y.; Arai, H.; Seiyama, T. *Sens. Actuators* **1985**, *7*, 11.
(2) Insley, R. U.S. Patent US 3995184, 1985.
(3) Adridge, C. L. U.S. Patent US 04456703, 1984.
(4) Busca, G.; Daturi, M.; Finocchion, E.; Lorenzelli, V.; Ramis, G.; Wiley: R. J. *Catal. Today* **1997**, *33*, 239.
(5) Valenzuela, M. A.; Jacobs, J. P.; Bosch, P.; Reijne, S.; Zapata, B.; Brongersma, H. H. *Appl. Catal., A* **1997**, *148*, 315.
(6) Busca, G.; Lorenzelli, V.; Sanchez Escribano, V. *Chem. Mater.* **1992**, *4*, 595.
(7) Roesky, R.; Weiguny, J.; Bestgen, H.; Dingerdissen, U. *Appl. Catal., A* **1999**, *176*, 213.
(8) Lee, J. M.; Baumann, W. C. U.S. Patent US 4446201, 1984.
(9) Luck, F. U.S. Patent US 51168001, 1992.
(10) Otero Aréan, C.; Penarroya Mentruit, M.; Escalona Platero, E.; Llabres i Xamena, F. X.; Parra, J. B. *Mater. Lett.* **1999**, *39*, 22.
(11) Escalona Platero, E.; Otero Aréan, C. *Res. Cem. Intermed.* **1999**, *25*, 187.
(12) Fujii, E.; Torii, H.; Takayama, R.; Hirao, T. J. *Mater. Sci.* **1995**, *30*, 6013.
(13) Stollberg, D. W.; Carter, W. B.; Hampikan, J. M. *Surf. Coat. Technol.* **1997,** *94-5*, 137.
(14) Corla, C. R.; Mayo W. E.; Liang, S.; Lu, Y. *J. Appl. Phys.* **2000**, *87*, 3736.
(15) Choi, Y. K.; Kim, B. H. *J. Ceram. Soc. Jpn.* **2000**, *108*, 261.
(16) Kim, M. K.; Chung, H. T. Um, W. S.; Park, Y. J.; Kim, J. G., Kim, H. G. *Mater. Lett.* **1999,** *39*, 133.
(17) Hyun, S. H.; Song, W. S. *J. Mater. Sci.* **1996**, *31*, 2457.
(18) Colyer, L. M.; Greaves, G. N.; Dent, A. J.; Carr, S. W.; Fox, K. K.; Jones, R. H. *Stud. Surf. Sci. Catal.* **1994**, *84*, 387.
(19) Colyer, L. M.; Greaves, G. N.; Dent, A. J.; Fox, K. K.; Carr, S. W.; Jones, R. H. *Nucl. Instr. Methods Phys. Res. B* **1995**, *97*, 107.
(20) Colyer, L. M.; Greaves, G. N.; Carr, S. W.; Fox, K. K. *J. Phys. Chem. B* **1997**, *101*, 10105.

10.1021/cm001138j CCC: $20.00
Published on Web 02/01/2001

Table 1. Specific Surface Areas (BET), Average Pore Sizes (BJH, Desorption), and Particle Sizes (from XRD Data and TEM) of Transition Metal Spinels Obtained at a Given Temperature (T_{calc}) from Transition Metal Doped Zeolites with Different Transition Metal to Aluminum Ratios (Me^{2+}/Al^{3+})

								d_{Part} (nm)	
sample	zeolite	exchanges	Me^{2+}/Al^{3+}	T_{calc} (°C)	spinel	A_{BET} (m^2/g)	d_{Pore} (nm)	XRD	TEM
1	Co−A	3	0.88	850	$CoAl_2O_4$	192	7.3	8	−
2	Co−A	5	1.06	850	$CoAl_2O_4$	147	5.9	10	12
3	Co−X	5	1.30	850	$CoAl_2O_4$	154	6.6	8	12
4	Co−Y	5	0.82	950	$CoAl_2O_4$	76	10.7	23	20
5	Ni−A	3	0.48	1100	$NiAl_2O_4$	104	9.5	13	−
6	Ni−A	5	0.67	1100	$NiAl_2O_4$	152	10.1	7	10
7	Ni−X	5	1.46	1100	$NiAl_2O_4$	104	10.2	8	12
8	Ni−Y	5	0.80	1100	$NiAl_2O_4$	124	9.4	7	10
9	Zn−A	5	0.53	1000	$ZnAl_2O_4$	76	9.5	24	−

(Co^{2+}, Ni^{2+}) or at room temperature (Zn^{2+}) for 30 min. The ion exchange was repeated up to four times to achieve high transition metal contents of the exchanged zeolites. Three different zeolites were used for the ion exchange, zeolite A ($Na_{12}Al_{12}Si_{12}O_{48}\cdot 20H_2O$, structure type LTA[21]), zeolite X ($Na_{78}K_{18}Al_{96}Si_{96}O_{384}\cdot 87H_2O$, structure type FAU[22]), and zeolite Y ($Na_{59}Al_{59}Si_{133}O_{384}\cdot 234H_2O$, structure type FAU). Zeolites A and X have the same Si/Al ratio, while zeolite X and Y crystallize in the same structure type with different Si/Al ratios. The transition metal salt solutions were prepared using $Co(NO_3)_2\cdot 6H_2O$ (99%, Fluka), $NiSO_4\cdot 6H_2O$ (98%, Riedel de Haën), and $ZnCl_2$ (98%, Fluka). After each ion exchange the solid material was filtered, washed with deionized water, and dried at 90°C in air.

The spinel particles crystallize during the calcination of transition metal exchanged zeolites. Calcination destroys the zeolites, and the spinels grow in the resulting amorphous silicate matrix. Therefore, the exchanged zeolites were heated at a rate of 5 °C min^{-1} to the temperatures given in Table 1. When the respective temperatures were reached, the samples were removed from the oven and quenched to room temperature. Repeated leaching of 0.5 g of the resulting solids in 100 mL of 1 NaOH solution at 90 °C for 10 h dissolved the amorphous silicate. The obtained spinel particles were separated by filtration and washed successively with 0.1 M NaOH solution, 0.1 M HCl solution, and water. The final products were dried at 90 °C.

To obtain more material, 50 g of zeolite was exchanged three times in 1000 mL of 0.25 M salt solutions and calcined to the respective temperatures. The resulting solids were leached several times in 1000 mL of 1 M NaOH solution and washed as described.

X-ray diffraction patterns were measured on a Stoe STADI P θ/θ diffractometer, equipped with a graphite monochromator mounted in front of a scintillation counter. For particle size calculations of the crystallites, LaB_6 (99%, Aldrich) was used to determine the instrumental broadening of the diffraction signals. The suitability of the LaB_6 was checked by comparing the fwhm of the X-ray reflections with those of a silicon standard material (NIST 640b). The calculations were performed with the software packet WinXPow[23] using the Scherrer equation to calculate the particle size broadening and the Wilson equation to calculate microstrain. A Johanna Otto HDK S1 high-temperature chamber was used on the same diffractometer for in situ high-temperature experiments. Samples were heated on a platinum support serving as a resistant heater to a final temperature of 1100 °C in air. To pursue phase transition processes, X-ray diffraction patterns were measured every 50 °C. Specific surface areas and the pore dimensions (voids) of the obtained materials were deduced from nitrogen adsorption/desorption isotherms measured at 77 K on a Micromeritics ASAP 2010 unit using the BET[24] and the BJH method.[25] All samples were outgassed under vacuum (4×10^{-3} mbar) at 300 °C for 6 h prior to the sorption measurements. The chemical composition of the obtained materials were determined by EDX analyses using an Oxford EDX unit attached to a Hitachi S-3500N scanning electron microscope. TEM images were obtained on a Hitachi 7500 and a Hitachi HF 2000 transmission electron microscope. The Hitachi HF2000 system was equipped with a Kevex Systems EDX unit.

Results

The amount of transition metal incorporated within a specific zeolite (A, X, or Y) is controllable by the number of ion exchange repetitions and the temperature of the exchange solutions. Detailed investigations on the ion exchange of the three zeolites with transition metal cations and on the stability of the exchanged zeolites are reported elsewhere.[26] The transition metal content of the exchanged zeolites considered in the present work are given in Table 1 (Me^{2+}/Al^{3+}). After five exchanges at 70 °C Co^{2+} and Ni^{2+} are over exchanged in all three zeolites. The overexchange is less pronounced with zeolite Y (samples 4 and 8). Obviously, the level of exchange in zeolite A and X can be reduced by using fewer exchange cycles. The Co^{2+}/Al^{3+} ratio of three times exchanged Co−A (sample 1) is much lower than that of five times exchanged Co−A (sample 2). All Co^{2+} and Ni^{2+} exchanged zeolites contain a nonnegligible amount of residual Na^+ cations which are not present in Zn^{2+}-exchanged zeolites. Not only does Zn^{2+} remove basically all the Na^+ within the zeolite but also it does not overexchange as Co^{2+} and Ni^{2+} do (see sample 9).

The structural frameworks of all exchanged zeolites collapse during calcination. The temperatures at which this occurs is dependent on the zeolite used, the exchanged cation, and the conditions used during ion exchange. During the exchange in acidic transition metal solutions, the zeolite frameworks are damaged leading to lower temperatures for complete structural collapse. The damage of the zeolite frameworks is enhanced after repeated ion exchanges. The framework of the siliceous zeolite Y is usually less affected by the exchanges than those of the low silica zeolites A and X. In situ X-ray diffraction experiments, as shown in Figure 1, reveal the collapse of the zeolite frameworks and the formation of an amorphous intermediate phase. The spinels grow as small particles in this amorphous

(21) Meier, W. M.; Olson, D. H.; Baerlocher, Ch. *Zeolites* **1996**, *12* (5), 96.
(22) Meier, W. M.; Olson, D. H.; Baerlocher, Ch. *Zeolites* **1996**, *12* (5), 122.
(23) *WinXPow 1.06*; Stoe & Cie: Darmstadt, Germany, 1999.
(24) Brunauer, S.; Emmet, P. H.; Teller, E. *J. Am. Chem. Soc.* **1938**, *60*, 309.
(25) Barret, E. P.; Joyner, L. G.; Halenda, P. H. *J. Am. Chem. Soc.* **1951**, *73*, 373.
(26) Weidenthaler, C.; Schmidt, W. *Chem. Mater.* **2000**, *12*, 3811.

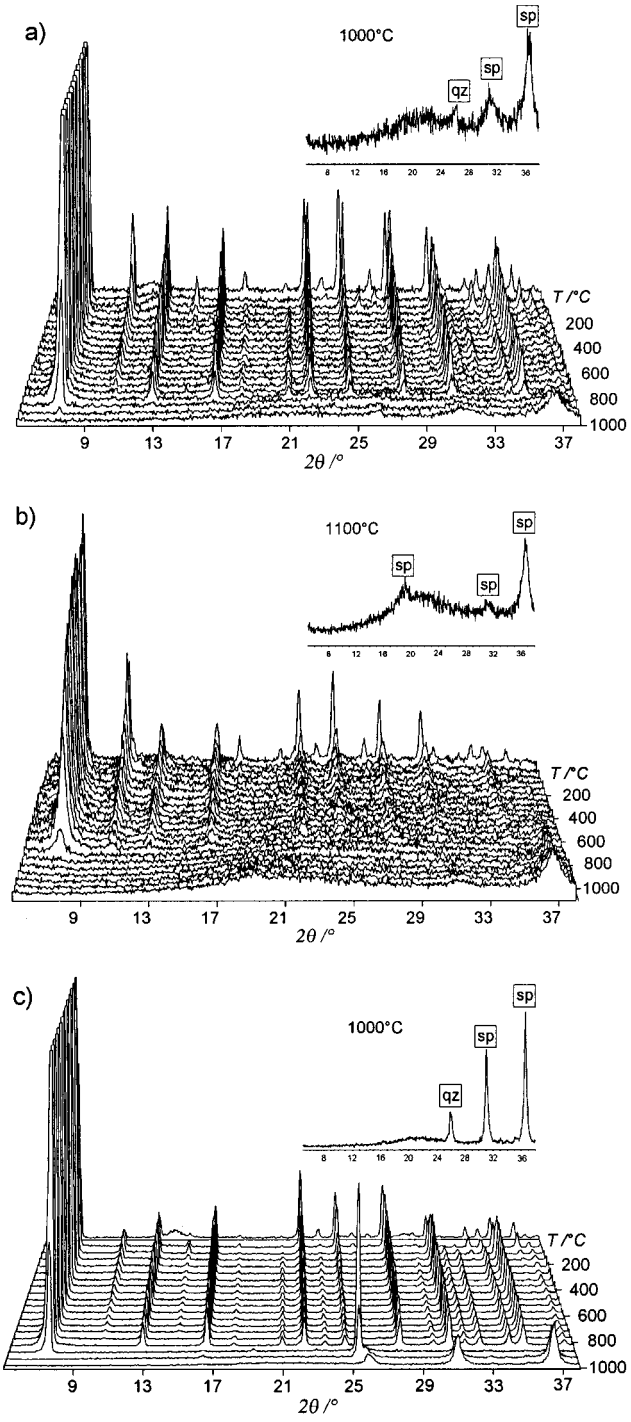

Figure 1. In situ high-temperature X-ray patterns of five times exchanged (a) Co^{2+}, (b) Ni^{2+}, and (c) Zn^{2+} zeolite A (sp = spinel, qz = quartz).

matrix, as shown by the broad reflections in Figure 1. The insertions show the enlarged diffraction patterns at the highest temperatures of the respective plots. The large amounts of amorphous materials cause broad signals between 10 and 30° in 2θ. Prolonged calcination and/or calcination at higher temperature leads to the formation of larger spinel crystallites indicated by the narrowing of the reflections as shown for a Ni−A sample in Figure 2. The spinel reflections become sharper with higher calcination temperatures (Figure 2a) and after the samples are kept at one temperature for 12 h (Figure 2b).

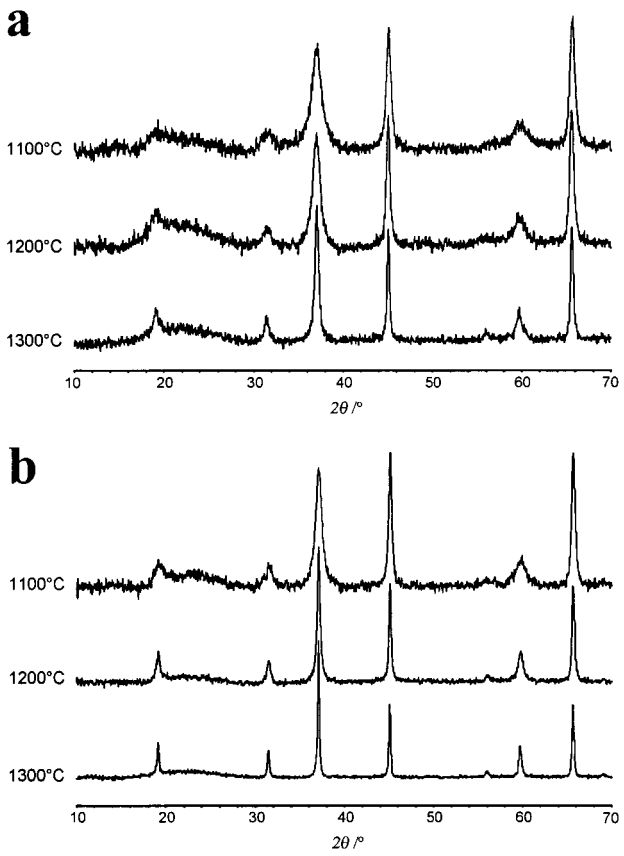

Figure 2. XRD patterns of $NiAl_2O_4$ samples from Ni−A which were (a) quenched after achieving 1100, 1200, and 1300 °C and (b) after 12 h at these temperatures. The narrowing of the reflections indicates larger particles.

During the calcination of the overexchanged zeolites Ni−A and Ni−X nickel oxide is formed as a crystalline intermediate phase immediately after the collapse of the zeolite frameworks, followed by the formation of the $NiAl_2O_4$ spinel. At higher temperature the nickel oxide dissolves in the solid matrix while the spinel remains stable. With Ni−Y, Co−A, Co−X, and Co−Y as precursors no other phases than spinels are formed. Zn−β quartz and mullite are observed with the $ZnAl_2O_4$ spinel. In addition to these phases willemite forms if Zn−X and Zn−A are used as precursors. These byphases decompose at higher temperature and quartz crystallizes (see Figure 1c) transforming into cristobalite at still higher temperatures. In most cases the choice of appropriate calcination conditions and temperatures permits the formation of solids with spinel as the only crystalline phase together with an amorphous byphase. The temperatures to which the solids were heated are given in Table 1 for various transition metal containing zeolites.

The solids which are obtained after the calcination have rather low specific surface areas of about 1−5 m^2 g^{-1}. The particle sizes of the spinels, calculated from the broadening of the X-ray reflections, would suggest much higher surface areas (see Table 1). The surfaces of the spinel particles are obviously not accessible. TEM micrographs show that the crystalline particles are completely covered by the amorphous matrix in which the particles crystallize (Figure 3a). Thus, the specific surface areas measured are those of the amorphous matrixes in which the nanosized spinel crystallites are

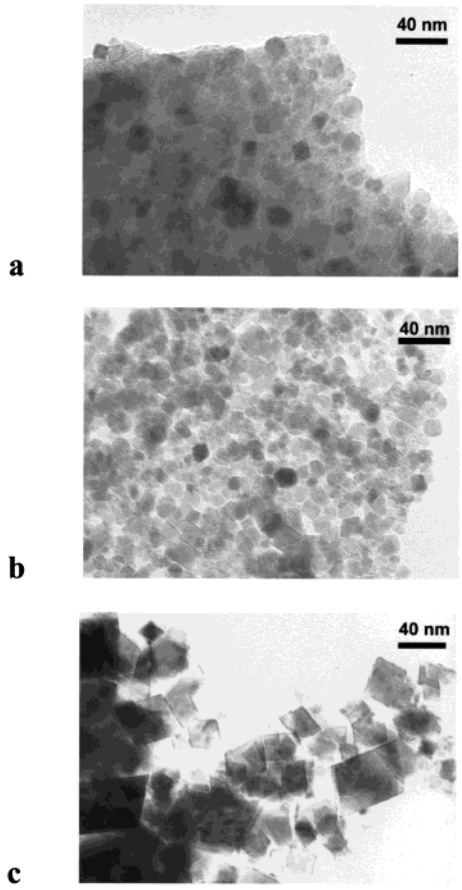

Figure 3. TEM micrographs of $NiAl_2O_4$ spinel particles from Ni−A (a) obtained at 1100 °C (particles embedded within the amorphous matrix), (b) obtained at 1100 °C after leaching procedure (individual particles), and (c) obtained at 1300 °C after leaching procedure.

embedded. The amorphous matrixes primarily contain silicate and in some cases (overexchange) a small amount of transition metal species as TEM/EDX data show. Since this matrixes are siliceous, they can be dissolved easily by treating the solids with sodium hydroxide solution at elevated temperature. Successive washing with NaOH solution and HCl solution after the leaching procedure removes all soluble silicate and excess transition metal species from the surface. Repetition of this procedure leads to a successive increase of the specific surface area of the obtained solid, as shown in Figure 4 for a Ni−A zeolite heated to 1100 °C (sample 5). The specific surface area of that sample increases from 2 $m^2\ g^{-1}$ of the as made material to 57 $m^2\ g^{-1}$ after one leaching procedure and 152 $m^2\ g^{-1}$ after two leaching procedures. The free particles obtained after two leaching procedures are shown in Figure 3b. Using small sample amounts, two or three leaching procedures are usually sufficient. Additional treatments with hot NaOH solution do not lead to any further increase of the specific surface area. However, if larger sample amounts are leached in small volumes of NaOH solution, the procedure has to be repeated several times to remove all of the amorphous silicate. By the leaching in alkaline solution, not only the amorphous silicate dissolves but also minor amounts of siliceous byphases dissolve as mullite, Zn−β quartz, or −willemite, which are formed from Zn^{2+}-doped zeolite precursors. Figure 5 shows the X-ray diffraction patterns of the pure

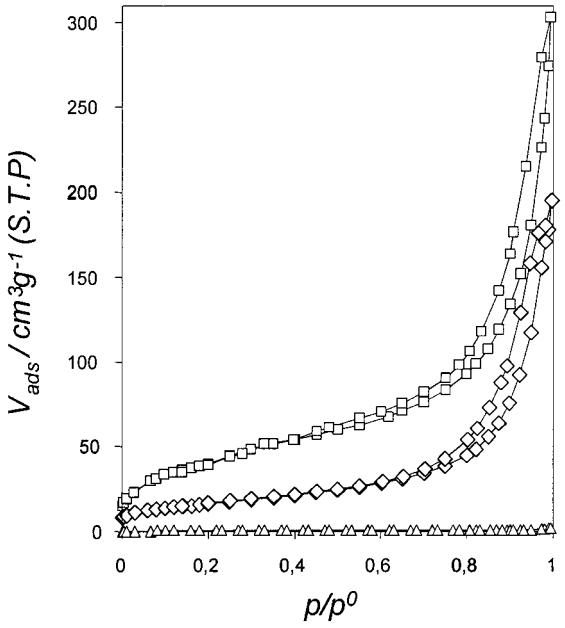

Figure 4. N_2 adsorption/desorption isotherms of Ni−A heated to 1100 °C, as made (2 $m^2\ g^{-1}$, triangles), after one leaching procedure (57 $m^2\ g^{-1}$, rhombs), and after two leaching procedures (152 $m^2\ g^{-1}$, squares).

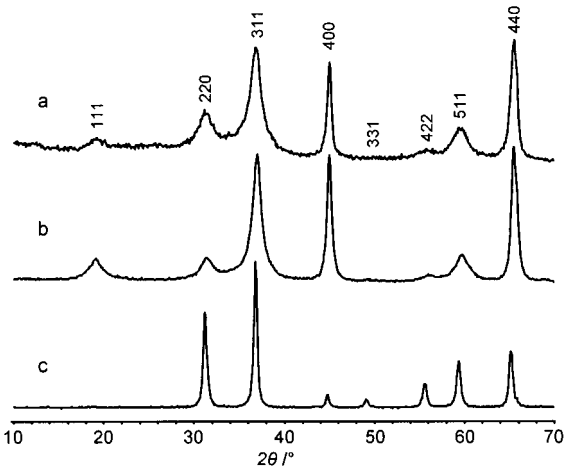

Figure 5. (a) $CoAl_2O_4$ (192 $m^2\ g^{-1}$), (b) $NiAl_2O_4$ (152 $m^2\ g^{-1}$), and (c) $ZnAl_2O_4$ (76 $m^2\ g^{-1}$) obtained after 2 leaching procedures from CoA (850 °C), Ni−A (1100 °C), and ZnA (1000 °C).

$CoAl_2O_4$, $NiAl_2O_4$, and $ZnAl_2O_4$ spinels obtained from transition metal exchanged zeolite A. Typically, the X-ray reflections are rather broad due to the small sizes of the spinel particles. The X-ray patterns of the spinels before and after the leaching procedures are identical. The crystal structures as well as the sizes and shapes of the spinel particles are obviously not affected by the leaching procedures which is also confirmed by TEM investigations.

The particle sizes of the obtained materials calculated by X-ray diffraction and measured by transmission electron microscopy are in fair agreement, showing that the domain sizes of the spinel crystallites correspond generally with the particle sizes. However, the calculation of the particle sizes from X-ray diffraction data turns out to be difficult for very small spinel particles. In the diffraction patterns of the small-sized spinels at least two types of broadening of different reflections are observed. Figure 5 shows that the 400 and 440 reflec-

tions of these $CoAl_2O_4$ and $NiAl_2O_4$ spinels are less broadened compared to the other reflections. Calculations of the particle sizes from the broader reflections lead to particle sizes much smaller than observed by TEM. Only the sharper reflections (e.g. 400 and 440) lead to particle sizes in the same range. These reflections seem to be broadened due to the small sizes of monocrystallites since HRTEM investigations show domains of lattice planes of the same size as the particle dimensions. The other reflections appear to be additionally broadened by other effects and should rather not be used to calculate particle sizes. Larger spinel particles lead to more uniformly broadened reflections which then can all be used for crystallite size calculations (e.g. $ZnAl_2O_4$, Figure 5) within the limits of the method (crystallites $\ll 1$ μm).[27] The reasons for the additional reflection broadening of very small transition metal spinels are not yet clear, but stacking faults and microstrain due to the thermal treatment might play a role.

The Me^{2+}/Al^{3+} ratios of the final products of generally 0.5 suggest pure spinel phases, and the yields imply that the aluminum is transferred almost quantitatively into the spinel phase. The nitrogen sorption isotherms of the pure spinel materials are all of the same shape as the one on top of Figure 4 indicating nonporous materials. The BET constants derived from the isotherms generally were in the range of 80 ± 10 allowing reliable determinations of the monolayer capacities.[28] The BET areas calculated from these values are listed in Table 1. The determined errors of the BET surfaces were less than $\pm 1\%$. The voids between the particles form an interparticle pore system with pore size distributions in the mesopore range. The mean diameters of the voids (d_{Pore}), determined from the desorption branch of the isotherms according to BJH, are also presented in Table 1.

Discussion

In zeolites the element distribution of framework atoms and guest atoms/cations is very uniform, since all elements are fixed at crystallographically defined sites. This perfect element distribution on an atomic scale enables a uniform nucleation of phases from the zeolite precursor. After the collapse of the zeolite framework, the element dispersion is maintained and the nucleation of dense phases starts homogeneously within the amorphous material. The growth rate of the crystallites depends on the reaction temperature. At higher temperatures the growth rate is enhanced. Therefore, larger crystallites are obtained either by prolongation of the reaction time or by applying higher temperatures (Figure 3b,c). The crystallization of every phase starts at a distinct temperature which depends on the system (transition metal, transition metal content, zeolite, etc.) and on the reaction conditions (heating rate, sample amount, calcination time, etc.). By adjustment of these parameters, the phase composition and the crystallite sizes can be varied. The choice of appropriate conditions leads to spinel particles with sizes in the nanometer range. In most cases the respective spinels can be obtained without any other crystalline byphase. The amorphous silicate matrix dissolves easily in hot alkaline solution. The remaining crystalline spinel particles can be separated either by filtration or centrifugation after washing successively with alkaline and acidic solution. Washing with alkaline solution removes residual soluble silicate species from the crystallite surfaces and acidic washing removes transition metal hydroxides formed during the alkaline treatment from excess transition metal. In most cases two or three leaching and washing steps are sufficient to obtain the pure transition metal spinels.

Due to the high specific density of the spinel materials ($CoAl_2O_4$, $\rho = 4.41$ g cm^{-3}; $NiAl_2O_4$, $\rho = 4.51$ g cm^{-3}; $ZnAl_2O_4$, $\rho = 4.60$ g cm^{-3}), the values of their specific surface areas are smaller than for silica or alumina particles of the same size. The specific surface areas of spherical 10 nm particles calculate as 273 m^2 g^{-1} for silica ($\rho = 2.2$ g cm^{-3}) compared to only 136 m^2 g^{-1} for $CoAl_2O_4$, 133 m^2 g^{-1} for $NiAl_2O_4$, and 130 m^2 g^{-1} for $ZnAl_2O_4$. These values are in good agreement with the dimensions calculated for the obtained spinel particles (Table 1, ABET and d_{Part}). Voids between particles form an interparticle pore system with pore dimensions typically smaller than the particles. Within the experimental error the pore diameters calculated by the BJH method agree quite well with this expectation (Table 1, d_{Pore}). The shape of the hysteresis of the nitrogen adsorption/desorption isotherms is of type H3 according to the IUPAC classification,[29] suggesting slit-shaped pores or aggregates of platelike particles. TEM images show that the voids between the particles are formed, more or less, by parallel crystallite surfaces with a rather broad void size distribution. The voids are large enough to give access to the surfaces of the particles which is of predominant importance for catalytic applications.

The presented preparation method for high surface area spinels has some advantages over the conventional methods. Zeolite precursors are inexpensive and easy to handle. During the calcination, no flammable vapors are produced as with the sol−gel method, and the silicate byphases are easily removable by alkaline leaching which is hardly possible with alumia byphases which are often obtained with the coprecipitation method. The preparation of spinels from transition metal exchanged zeolites is easy to control and reproducible. The specific surface areas of the obtained materials are those of the pure spinels.

Conclusions

Transition metal exchanged zeolites are valuable precursor materials for nanosized transition metal spinels. Due to the high dispersion of the elements within the matrix, formed by the collapse of a zeolite precursor, the nucleation of the spinel crystallites occurs simultaneously within the whole solid. High temperatures enable the ion diffusion within the matrix, but its

(27) Jenkins, R.; Snyder, R. L. *Introduction to X-ray Powder Diffractometry*; Chemical Analysis, Vol. 138; Winefordner, J. D., Ed.; J. Wiley & Sons: New York, 1969.

(28) Rouquerol, F.; Rouquerol. J.; Sing, K. *Adsorption by Powders and Porous Solids*; Academic Press: London, 1999.

(29) Sing, K. S. W.; Everett, D. H.; Haul, R. A. W.; Moscou, L.; Pierotti, R. A.; Rouquerol, J.; Siemieniewska, T. *Pure Appl. Chem.* **1985**, *57* (4), 603.

solid nature slows down the diffusion rate. Thus, the particles grow rather slowly within the amorphous solid matrix. Quenching the reaction solid to room temperature at appropriate temperatures and reaction times enables a degree of control over the crystal growth, and thus, particle size is controllable. By dissolution of the amorphous matrix, the spinel particles with the desired particle sizes are accessible. Since the reaction matrix is an amorphous silicate, it is easily removable with alkaline solution, an advantage over other routes where insoluble crystalline or amorphous byphases as aluminum oxides occur (e.g. coprecipitation or sol gel route). Nanoscaled spinel particles with high surface areas are obtained by this novel preparation route, without the formation of byphases. Due to their high surface area and stability these materials are predefined as catalyst supports and/or as catalysts themselves. Not only can ternary oxides such as the above spinels be obtained by this method but also quaternary oxides (e.g. mixed transition metal aluminates) using zeolites which are exchanged simultaneously with two different transition metals. In general, the basic strategy of the described preparation of high surface materials is not only limited to spinels but also transferable to other materials (e.g. other metal aluminates) that form from zeolites or other host−guest precursors.

Acknowledgment. We thank Mr. Bongard, Mr. Spliethoff, Mr. Dreier, and Dr. Tesche for EDX and TEM analyses, Dr. Tissler (AlSiPenta) for providing the zeolites, and the Deutsche Forschungsgemeinschaft (Schm936/3-1) for financial support.

CM001138J